

## Electrical Transport Properties and Electronic Structure of Transparent Conductive Oxides with Delafossite Structure

Hiroshi Yanagi, Kazushige Ueda and Hideo Hosono

Materials and Structures Laboratory, Tokyo Institute of Technology,  
4259 Nagatsuta, Midori-ku, Yokohama 226-8503, Japan  
Fax: 81-45-924-5339, e-mail: h-yanagi@rlem.titech.ac.jp

Transparent conductive oxides with delafossite structure show promise for the fabrication of transparent semiconductor devices. Thin films of delafossite-type oxides were prepared by PLD method on sapphire substrates. The  $\text{CuAlO}_2$  and  $\text{CuGaO}_2$  thin films exhibited  $p$ -type conduction. The dc conductivity at R.T. was  $0.3 \text{ S cm}^{-1}$  for  $\text{CuAlO}_2$  or  $0.06 \text{ S cm}^{-1}$  for  $\text{CuGaO}_2$ . On the other hand, the thin films of  $\text{AgInO}_2:\text{Sn}$  exhibited  $n$ -type conduction. The dc conductivity of  $\text{AgInO}_2:\text{Sn}$  thin films at R.T. was  $70 \text{ S cm}^{-1}$ . Contribution of Cu  $3d$  components to upper edge of valence band in  $\text{CuAlO}_2$  was confirmed by photoemission spectroscopic measurements. The present results supported our working hypothesis for chemical design of  $p$ -type conducting transparent oxides.

Key words: TCO,  $p$ -type conductor, delafossite, PLD, photoemission spectroscopy

### 1. INTRODUCTION

Transparent conductive oxides (TCOs) such as electron doped  $\text{ZnO}$ ,  $\text{In}_2\text{O}_3$ ,  $\text{SnO}_2$  are widely and practically used as transparent electrodes in flat panel displays, solar cells and touch panels. However, all conduction type of these materials is  $n$ -type, no  $p$ -type TCO was found so far. This mono-polarity is the primary origin of the restricted application of TCOs. Therefore, realization of  $p$ -type TCOs should be a milestone to expand the utilization of TCOs as transparent oxide semiconductors, because a wide variety of active functions of semiconductor devices comes from  $p$ - $n$  junctions.

We have proposed a guideline for chemical design of  $p$ -type TCOs and found  $\text{CuAlO}_2$  [1-3],  $\text{CuGaO}_2$  [3] and  $\text{SrCu}_2\text{O}_2$  [4] as a consequence of exploration efforts following the guideline. Further, Transparent  $p$ - $n$  heterojunction diodes,  $p$ - $\text{SrCu}_2\text{O}_2$  /  $n$ - $\text{ZnO}$ , with rectifying and UV-emitting functions have been successfully fabricated [5, 6]. In order to achieve better performance, fabrication of  $p$ - $n$  heterojunctions with same crystal structure is desirable. Transparent oxides with delafossite structure are unique materials that satisfy our working hypotheses for exploring both  $p$ - and  $n$ -type TCOs. It turned out that  $\text{CuAlO}_2$  and  $\text{CuGaO}_2$  delafossites are  $p$ -type TCOs, while Sn doped  $\text{AgInO}_2$  delafossite is  $n$ -type TCO [7, 8].

Our guideline to find  $p$ - and  $n$ -type TCOs are summarized in as follows [1, 9]: The essence of guideline to find  $p$ -type TCOs is to have monovalent copper as the major constituents. The selection of  $\text{Cu}^+$  is based on its electronic configuration and energy levels of  $3d$  orbitals. Cuprous ion has the electronic configuration of  $(\text{Ar}) 3d^{10}4s^0$  (closed shell), which is free from visible coloration arising from a  $d$ - $d$  transition commonly seen in transition metal ions. The energy

level of a  $3d^{10}$  state is close to that of an  $\text{O } 2p^6$  state. As a consequence, covalent bonding formation or hybridization of orbitals is expected between Cu  $3d^{10}$  and O  $2p^6$ . The hybridization of the orbitals will bring large dispersion to the valence band or reduction of the localization of positive holes. Formation of a covalent bonding between  $\text{Cu}^+$  and  $\text{O}^{2-}$  ions demands an appropriate crystal structure. The crystal structure is required to meet two requirements, one is that  $\text{Cu}^+-\text{O}^{2-}$  bonds with a moderated covalency exist, and another is to retain a wide energy gap for optical transparency. This argument can be valid also to  $\text{Ag}^+$  instead of  $\text{Cu}^+$ .

For the  $n$ -type TCO, high mobility of carrier electron in the conduction band is required. A linear chain of edge-sharing octahedra, in which the  $p$ -block heavy cations ( $\text{M}^{+}$ ) with  $ns^0$  electric configuration ( $n$ : the principal quantum number) occupy the central position, is preferred to satisfy this requirement. Since there is no intervening oxygen between the two neighboring M cations in the chain of edge-sharing octahedra, direct overlap between  $ns$  atomic orbitals of the neighboring M cations is possible for the  $p$ -block heavy cations. In this case, the bottom edge of conduction band is mainly composed of  $ns$  atomic orbitals of M cations. As a consequent, a large dispersion of the conduction band, which is appropriate for high mobility of electron carrier, may be expected.

Taking the above stated requirements into consideration, we selected as the candidate materials ternary noble metal oxide with delafossite structure ( $\text{ABO}_2$ ). Figure 1 illustrates delafossite-type crystal structure. The delafossite is composed of an alternate stacking O-A-O dumbbells and  $\text{BO}_6$  edge-sharing octahedral layer. According to our hypothesis, delafossite oxides satisfy the requirements for  $p$ - and  $n$ -type TCOs,

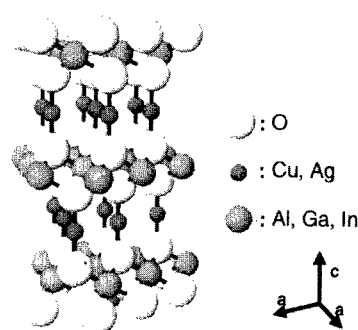


Fig. 1. Crystal structure of delafossite ( $ABO_3$ ). This material has layer structure composed of A (A = Cu, Ag) plane and  $BO_3$  (B = Al, Ga, In) layer alternately stacked along  $c$ -axis.

when Cu and/or Ag as A cation and  $p$ -block heavy cations, such as  $Ga^{3+}$  and  $In^{3+}$ , as B cation are chosen. It is considered that  $BO_6$  octahedral layers and O–A–O layers work as conduction paths for electrons and positive holes, respectively. That is to say, double oxides with delafossite structure are candidate materials for preparing  $p$ - and  $n$ -type TCOs aiming at a transparent  $p$ - $n$  junction using the same crystal structure.

The present paper describes (1) the preparation of  $p$ -type conducting  $CuAlO_2$  and  $CuGaO_2$  thin films and  $n$ -type conducting  $AgInO_2$  thin films by pulsed laser deposition (PLD) method [10] and (2) the electric structure of  $CuAlO_2$ , which is a prototype of  $p$ -type conducting transparent oxides, probed by photoemission spectroscopy.

## 2. EXPERIMENTAL

Polycrystalline  $CuAlO_2$  was synthesized by heating a stoichiometric mixture of  $Cu_2O$  and  $Al_2O_3$  at 1373 K for 10 h [11]. The powder was pressed into a pellet by a cold isostatic press (CIP) at  $800 \text{ kg cm}^{-2}$  and then sintered at 1373 K for 10 h. Resulting sintered pellets were used as the target for preparation of  $CuAlO_2$  thin films by PLD method.

Sintered pellets of  $CuGaO_2$  for the target PLD were prepared by using solid state reactions of  $Cu_2O$  and  $Ga_2O_3$  [12]. Stoichiometric amounts of the raw materials were mixed thoroughly with methanol and calcined at 1373 K for 24 h. The material was pelletized, CIPed and sintered at 1373 K for 24 h.

$AgInO_2$  delafossite were prepared by cation exchange reaction [13].  $NaInO_2$  with rock salt structure was first prepared by direct solid state reaction between  $Na_2CO_3$  and  $In_2O_3$  at 1123 K for 12 h in  $O_2$  gas flow. Then  $NaInO_2$  powder was mixed with  $AgNO_3$  and  $KNO_3$  in the molar ratio 1:1.8:0.8, and heated at 453 K for 48 h in air. Under the heat treatment,  $NaInO_2$  was subjected to the cation exchange of  $Na^+$  with  $Ag^+$  in the melt and as a consequent  $AgInO_2$  with delafossite structure was synthesized. The solidified mixture was washed with water to dissolve the remaining nitrates. In the preparation of targets for PLD, substitution of Sn 5 at.% with In was carried out to dope carrier electrons by using Sn doped  $NaInO_2$  in the cation exchange reaction [7], because non-doped  $AgInO_2$  sintered disks were almost insulating. Since this substitution was successful to enhance the conductivity in the disks, fabrication of

Table I Preparation condition for  $CuAlO_2$ ,  $CuGaO_2$  and  $AgInO_2$  thin films.

	$CuAlO_2$	$CuGaO_2$	$AgInO_2$
Target (pellet)	$CuAlO_2$	$CuGaO_2$	$AgInO_2$ , Sn
Substrate	$\alpha$ - $Al_2O_3$ (001)	$\alpha$ - $Al_2O_3$ (001)	$\alpha$ - $Al_2O_3$ (001)
Substrate-target distance (mm)	25	25	30
Substrate temperature (K)	963	973	723
Oxygen pressure (Pa)	1.3	9	13
KrF excimer laser			
Repetition frequency (Hz)	20	20	2
Energy density ( $J \text{ pulse}^{-1} \text{ cm}^{-2}$ )	5.0	6.0	8.0
Post annealing (h)	3	-----	-----

$AgInO_2$  thin films by PLD was performed using these disks as targets.

Thin films of  $CuAlO_2$ ,  $CuGaO_2$  and  $AgInO_2$  were deposited on  $\alpha$ - $Al_2O_3$  single crystal substrate by PLD method using KrF excimer laser (Lambda Physik Compex 102). The base pressure before the deposition was  $\sim 10^{-6}$  Pa. Table I summarizes the optimized preparation conditions for each thin film. The films of  $CuAlO_2$  were post-annealed at 963 K for 3 h after deposition, and were cooled down to room temperature maintaining an atmosphere oxygen partial pressure of 1.3 Pa.

Crystalline phases in the pellets and the films were identified by X-ray diffractometer (XRD) ( $Cu K\alpha$ , Rigaku Rint-2500), and film thickness was measured with a stylus (Sloan DEKTAK<sup>3</sup>ST). Optical transmission spectra of the films were measured with a dual beam spectrophotometer (Hitachi U-4000). Electrical conductivity was measured by the two-probe method in a temperature range 10 K ~ 300 K. Measurements of the Seebeck and Hall coefficients were carried out at room temperature.

Measurements of photoemission spectroscopy (PES) and inverse photoemission spectroscopy (IPES) were performed on the thin film samples at room temperature using an instrument built up in our laboratory. In the PES measurement, two excitation lights, He II resonance radiation (40.8 eV) and Mg  $K\alpha$  X-ray (1254 eV), were used for UPS and XPS, respectively. IPES spectra were measured in BIS mode by monitoring the intensity of emitting photon at 9.45 eV. These measurements were carried out under the vacuum level  $1 \times 10^{-7} \sim 5 \times 10^{-8}$  Pa.

## 3. RESULTS

Figure 2 shows XRD patterns of thin films and powders of the  $CuAlO_2$ ,  $CuGaO_2$  and Sn doped  $AgInO_2$ . All diffraction peaks were indexed as delafossite structure except for peaks from the substrate. The  $CuAlO_2$  and  $CuGaO_2$  thin films have orientation  $c$ -axis. Epitaxial growth of  $CuGaO_2$  was confirmed by X-ray pole figure and in-plane measurements, and its detail will be reported elsewhere [14].

Figure 3 shows optical transmission spectra of the  $CuAlO_2$ ,  $CuGaO_2$  and Sn doped  $AgInO_2$  thin films in visible and near infrared (NIR) regions. No distinct optical absorption band was observed in the visible region. Relatively high transmittance,  $\sim 70\%$  at 500 nm, was achieved for all films deposited under the optimized preparatory conditions. The direct allowed optical band gaps of  $CuAlO_2$ ,  $CuGaO_2$  and  $AgInO_2$  thin films are listed in Table II. In the spectrum of Sn doped  $AgInO_2$  thin film, a decrease in NIR ( $> 2000 \text{ nm}$ ) is due to the absorption by carrier electrons.

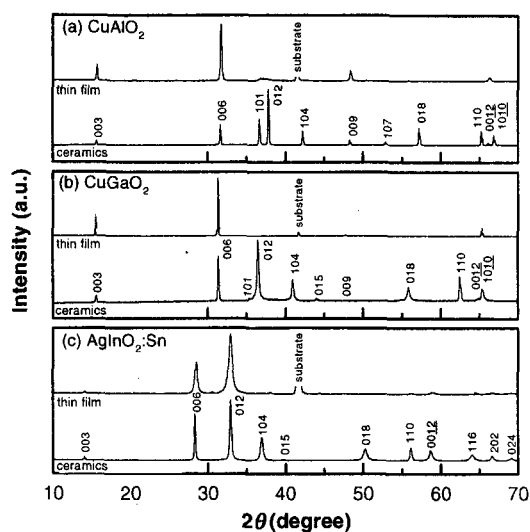


Fig. 2. XRD patterns of delafossites, CuAlO<sub>2</sub> (a), CuGaO<sub>2</sub> (b) and Sn doped AgInO<sub>2</sub> (c). Top and bottom pattern of each material are due to thin film and ceramics (for PLD target), respectively.

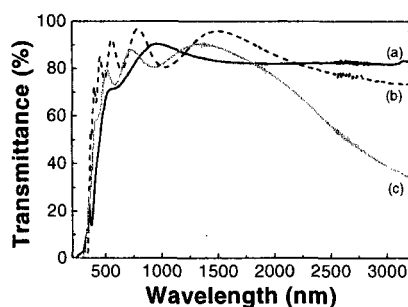


Fig. 3. Optical transmission spectra of CuAlO<sub>2</sub> (a), CuGaO<sub>2</sub> (b) and Sn doped AgInO<sub>2</sub> (c) thin films. The surface reflection loss of sapphire substrate was subtracted.

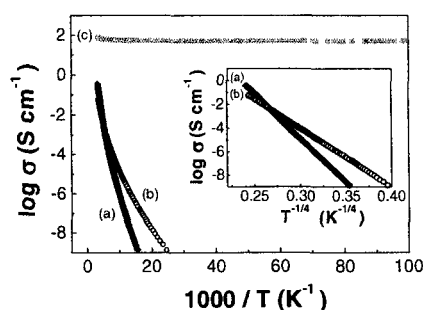


Fig. 4. Arrhenius plots of dc electrical conductivity in CuAlO<sub>2</sub> (a), CuGaO<sub>2</sub> (b) and Sn doped AgInO<sub>2</sub> thin films. Inset shows plots of  $\log \sigma$  vs.  $T^{-1/4}$  in CuAlO<sub>2</sub> and CuGaO<sub>2</sub> films.

Figure 4 shows temperature dependence of electrical conductivity in the CuAlO<sub>2</sub>, CuGaO<sub>2</sub> and Sn doped AgInO<sub>2</sub> thin films. Table II summarizes optical and electrical properties of these films at room temperature. The dc conductivities of the CuAlO<sub>2</sub> and CuGaO<sub>2</sub> thin films at room temperature were  $3.4 \times 10^{-1} \text{ S cm}^{-1}$  and  $6.3 \times 10^{-2} \text{ S cm}^{-1}$ , respectively. The temperature dependence of conductivities of the CuAlO<sub>2</sub> and

Table II. Optical and electrical properties of CuAlO<sub>2</sub>, CuGaO<sub>2</sub> and Sn doped AgInO<sub>2</sub> thin films at room temperature.

		CuAlO <sub>2</sub>	CuGaO <sub>2</sub>	AgInO <sub>2</sub> :Sn
Optical band gap	(eV)	~3.5	~3.6	~4.1
DC electrical conductivity	(S cm <sup>-1</sup> )	$3.4 \times 10^1$	$6.3 \times 10^2$	$7.3 \times 10^1$
Activation energy	(eV)	0.22	0.13	-----
Hall coefficient	(cm <sup>3</sup> C <sup>-1</sup> )	$+2.3 \times 10^{-1}$	+3.7	$-1.9 \times 10^{-2}$
Carrier density	(cm <sup>-3</sup> )	$2.7 \times 10^{19}$	$1.7 \times 10^{18}$	$3.3 \times 10^{20}$
Hall mobility	(cm <sup>2</sup> V <sup>-1</sup> s <sup>-1</sup> )	0.13	0.23	1.4
Seebeck coefficient	(μVK <sup>-1</sup> )	$+2.1 \times 10^2$	$+5.6 \times 10^2$	$-5.1 \times 10^1$

CuGaO<sub>2</sub> films may be described by Arrhenius type behavior near room temperature and the activation energy is estimated as 0.22 eV for CuAlO<sub>2</sub> or 0.13 eV for CuGaO<sub>2</sub>. On the other hand, the data on plots of  $\log \sigma$  vs.  $T^{-1/4}$  at low temperature region suggested that a variable-range hopping mechanism is dominant in this region. In the case of the Sn doped AgInO<sub>2</sub> thin film, no remarkable dependence of the conductivity on temperature was observed except for at higher temperatures near room temperature, indicating that the Fermi level of the specimen locates at above of the conduction band bottom. The Seebeck and Hall coefficients of the CuAlO<sub>2</sub> and CuGaO<sub>2</sub> were positive, indicating positive holes are undoubtedly major carriers in these thin films. On the other hand, the Seebeck and Hall coefficients of the Sn doped AgInO<sub>2</sub> was negative. Therefore we conclude that AgInO<sub>2</sub>:Sn thin films are *n*-type conductors.

XPS, UPS, and IPES spectra of CuAlO<sub>2</sub> thin film are shown in figure 5. Fermi energy determined experimentally was set as zero on the binding energy scale in the three spectra. The intensity of IPES was adjusted to be comparable to those of the PES spectra. The band gap, which was directly observable between the valence band edge in the PES spectra and the conduction band edge in the IPES spectrum, was ~3.5 eV. This value is in a reasonable agreement with the band gap evaluated by the optical measurement. The Fermi energy lies around the top of the valence band. This observation agrees with the fact that the specimen exhibits *p*-type electrical conductivity. A clear band was resolved at ~4 eV (band A) in the XPS spectrum. On the other hand, a broad band at ~7 eV (band B) and a shoulder at ~4 eV (band A) were observed in the UPS spectrum. In the IPES spectrum, a very broad band, which is indexed as X, was observed. No other band was resolved in the unoccupied state.

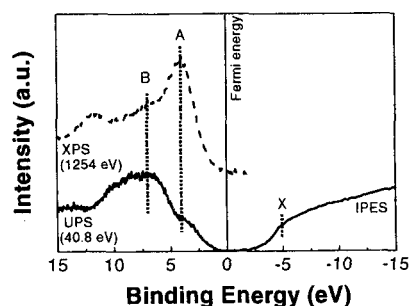


Fig. 5. PES and IPES spectra of CuAlO<sub>2</sub> thin film. The origin of the energy axis is Fermi level which was determined by using Au deposited on sample. Bands A, B and X are

#### 4. DISCUSSION

In this article, we described the detailed preparation procedure of *p*-type and *n*-type TCOs with delafossite structure. These materials described here, CuAlO<sub>2</sub>, CuGaO<sub>2</sub> and AgInO<sub>2</sub>, were found for the first time by us on the basis of our guideline. Here, we discuss the material selection toward the realization of transparent *p-n* junction using delafossite TCOs.

The candidate material for transparent *n*-type conductor with delafossite structure is only AgInO<sub>2</sub>, but there are two candidates for *p*-type; CuAlO<sub>2</sub> and CuGaO<sub>2</sub>. Both CuAlO<sub>2</sub> and CuGaO<sub>2</sub> delafossites thin films were oriented *c*-axis, however CuGaO<sub>2</sub> thin films were epitaxially growth in an as-deposited states [14]. This is an advantage for CuGaO<sub>2</sub> thin films to fabricate *p-n* junction, because epitaxial growth is expected to reduce structural imperfections at the *p-n* interface. The distances between neighboring oxygen ions on *c*-surface for CuGaO<sub>2</sub> and AgInO<sub>2</sub> are 0.298 nm and 0.328 nm, respectively, and this lattice mismatch is ~10%. On the other hand, the distances for CuAlO<sub>2</sub> and  $\alpha$ -Al<sub>2</sub>O<sub>3</sub> substrates are 0.286 nm and 0.252-0.287 nm, respectively, and the mismatch between AgInO<sub>2</sub> and CuAlO<sub>2</sub> is ~13%. Therefore, CuGaO<sub>2</sub> is expected to be more appropriate for combination than CuAlO<sub>2</sub>. Furthermore, an advantage of CuGaO<sub>2</sub> is that the oxygen pressure during deposition of CuGaO<sub>2</sub> is closed to that of AgInO<sub>2</sub>. This may be effective to prevent the oxidation of *p*-layer, which is needed to be deposited on sapphire before the deposition of AgInO<sub>2</sub> so as to obtain good crystal quality. The advantage of CuAlO<sub>2</sub> is higher electrical conductivity than that of CuGaO<sub>2</sub>. However, the conductivity of CuGaO<sub>2</sub> thin films will be enough to fabricate *p-n* junction to realize rectifying properties, because the conductivity of SrCu<sub>2</sub>O<sub>2</sub> layer in *p*-SrCu<sub>2</sub>O<sub>2</sub>/*n*-ZnO heterojunction exhibiting good rectifying properties, was 10<sup>-3</sup> S cm<sup>-1</sup>.

Next, the electronic structure on CuAlO<sub>2</sub> is discussed on the results obtained here. The structure of the upper part of valence band of CuAlO<sub>2</sub> was probed by UPS and XPS. It was found that the relative intensity of the band A with respect to band B increased largely in the XPS spectrum in comparison with the UPS spectrum. The ratios of emission cross section of Cu 3*d* electron to O 2*p* electron for 40.8 eV excitation and for 1254 eV excitation are ~1.5 and ~30 [15], respectively. Therefore, the change in the relative intensity of band A with varying excitation energies indicates that the contribution of Cu 3*d* to the upper valence band is significant. In most transparent oxides, the upper valence band is almost entirely composed of O 2*p* orbitals and the contribution metal cation's orbitals is not significant. This makes a sharp contrast with the nature of present material. As a consequence, it is now concluded that our chemical design to find a new TCO exhibiting *p*-type conductivity [1] is valid in the viewpoints of electronic structure.

#### 5. CONCLUSIONS

Thin films of CuAlO<sub>2</sub>, CuGaO<sub>2</sub>, and Sn doped AgInO<sub>2</sub> with delafossite structure were prepared by PLD

method on  $\alpha$ -Al<sub>2</sub>O<sub>3</sub> (001) as a first step to fabricate transparent homo-structural *p-n* junction. The conclusions obtained are summarized as follows.

- (1) CuAlO<sub>2</sub> and CuGaO<sub>2</sub> thin films oriented *c*-axis were obtained. No preferential orientation was seen for AgInO<sub>2</sub> thin films.
- (2) The Seebeck and Hall coefficients of the CuAlO<sub>2</sub> and CuGaO<sub>2</sub> were positive, while those of the Sn doped AgInO<sub>2</sub> were negative. Therefore CuAlO<sub>2</sub> and CuGaO<sub>2</sub> were *p*-type conductor and AgInO<sub>2</sub> was *n*-type one.
- (3) Photoemission spectroscopy revealed that the upper valence band of CuAlO<sub>2</sub> consist of Cu 3*d* orbitals to a large degree. This result provided a solid basis for our working hypotheses to explore *p*-type transparent oxides.

#### REFERENCES

- [1] H. Kawazoe, M. Yasukawa, H. Hyodo, M. Kurita, H. Yanagi, and H. Hosono, *Nature*, **389**, 939-42 (1997).
- [2] H. Yanagi, S. Inoue, K. Ueda, H. Kawazoe, and H. Hosono, *J. Appl. Phys.*, **88**, 4159-63 (2000)
- [3] H. Yanagi, H. Kawazoe, A. Kudo, M. Yasukawa, and H. Hosono, *J. Electroceram.*, **4**, 427-41 (2000)
- [4] A. Kudo, H. Yanagi, H. Hosono, and H. Kawazoe, *Appl. Phys. Lett.*, **73**, 220-22 (1998).
- [5] A. Kudo, H. Yanagi, K. Ueda, H. Hosono, H. Kawazoe, and Y. Yano, *Appl. Phys. Lett.*, **75**, 2851-53 (1999).
- [6] H. Ohta, K. Kawamura, M. Orita, N. Sarukura, M. Hirano and H. Hosono, *Electro. Lett.*, **36**, 984-85 (2000); H. Ohta, K. Kawamura, M. Orita, M. Hirano, N. Sarukura, and H. Hosono, *Appl. Phys. Lett.*, **77**, 475-47 (2000).
- [7] T. Otabe, K. Ueda, A. Kudoh, H. Hosono, and H. Kawazoe, *Appl. Phys. Lett.*, **72**, 1036-38 (1998).
- [8] S. Ibuki, H. Yanagi, K. Ueda, H. Kawazoe, and H. Hosono, *J. Appl. Phys.*, **88**, 3067-69 (2000)
- [9] H. Kawazoe, N. Ueda, H. Un'no, H. Hosono, and H. Tanoue, *J. Appl. Phys.*, **76**, 7935-41 (1994)
- [10] "Pulsed Laser Deposition of Thin Films", edited by D. B. Chrisey and G. K. Hubler Wiley-Interscience, New York, (1994).
- [11] T. Ishiguro, A. Kitazawa, N. Mizutani, and M. Kato, *J. Solid State Chem.*, **40**, 170 (1981)
- [12] K. T. Jacob, and C. B. Alcock, *Rev. int. Htes. Temp. et Refract.*, **13**, 37 (1976).
- [13] R. D. Shannon, D. B. Rogers, and C. T. Prewitt, *Inorg. Chem.*, **10**, 713 (1971); Y. J. Shin, J. P. Doumerc, P. Dordor, C. Delmas, M. Pouchard, and P. Hagenmuller, *J. Solid State Chem.*, **107**, 303 (1993)
- [14] K. Ueda, T. Hase, H. Yanagi, H. Kawazoe, H. Hosono, H. Ohta, M. Orita, and M. Hirano, *J. Appl. Phys.*, (in press)
- [15] J. -J. Yen, "Atomic Calculation of Photoionization Cross-Sections and Asymmetry Parameters", Gordon and Breach Science Publishers, Pennsylvania, (1993)